EUROPEAN TRANSACTIONS ON TELECOMMUNICATIONS
Eur. Trans. Telecomms. (2008)
Published online in Wiley InterScience
(www.interscience.wiley.com) DOI: 10.1002/ett.1273

Transmission Systems

Analysis of the narrowband interference effect on frequency ambiguity resolution for OFDM systems

Mohamed Marey* and Heidi Steendam†

DIGCOM Research Group, TELIN Department, Ghent University, Sint-Pietersnieuwstraat 41, 9000 Gent, Belgium

SUMMARY

In orthogonal frequency division multiplexed (OFDM) systems affected by carrier frequency offsets, frequency ambiguity resolution, i.e. the estimation of the part of the frequency offset corresponding to an integer times the carrier spacing is a crucial issue. The proper action of frequency ambiguity resolution algorithms can be strongly affected by the presence of disturbances, like narrowband interference (NBI). In this paper, the susceptibility of the blind and data aided maximum likelihood (ML) frequency ambiguity estimators to NBI signals, which may arise in the OFDM band as the spectrum becomes more crowded, is investigated in an analytical way. The analytical results are verified by means of simulations. Although the estimators turn out to be essentially independent of the bandwidth of the interferers and the number of interferers, the performance of the estimators is very sensitive to the positions of the interferers when the interferers are strong. Copyright © 2008 John Wiley & Sons, Ltd.

1. INTRODUCTION

Orthogonal frequency division multiplexing (OFDM) is widely known as a promising communication technique in broadband wireless mobile communication systems due to the high spectral efficiency and robustness to multi-path interference. Currently, OFDM has been adapted to digital audio and video broadcasting (DAB/DVB), high speed wireless local area networks (WLAN's) such as IEEE802.11x, HIPERLAN II, multimedia mobile access communication (MMAC), and multi-band OFDM type ultra-wideband (MB-OFDM UWB), etc. [1–3]. The principle weakness of OFDM is its sensitivity to carrier frequency offset (CFO) caused by Dopper shifts and/or oscillator instabilities [4]. A CFO results in a shift of the received signal spectrum in the frequency domain. The CFO can be divided into an integer and a fractional part with respect to the OFDM subcarrier spacing δf. If the integer part of the CFO equals I and the fractional part is zero, then the received subcarriers are shifted by $I \cdot \delta f$ in the frequency domain; the subcarriers are still mutually orthogonal, but the received data symbols, which are mapped to the OFDM spectrum, are in the wrong positions in the demodulated spectrum, resulting in a frequency ambiguity. This frequency ambiguity results in a BER of 0.5 [5] and must therefore be estimated and corrected.

Recently, new spectrum management strategies have been proposed [6, 7] which allow two systems to share the same frequency band. The broadband very high frequency (B-VHF) project, which aims to develop a new integrated broadband VHF system for aeronautical voice and data link communications based on multi-carrier technology is a good example of an overlay system [8–10]. In this project, the multi-carrier (MC) system is intended to share the parts of the VHF spectrum that are currently used by narrowband (NB) systems such as voice DSB-AM signal and VHF digital links. These NB systems are considered

* Correspondence to: Mohamed Marey, DIGCOM Research Group, TELIN Department, Ghent University, Sint-Pietersnieuwstraat 41, 9000 Gent, Belgium. E-mail: mohamed@telin.ugent.be
† Senior Member of IEEE.

Received 16 August 2006
Revised 26 February 2007
Accepted 15 November 2007

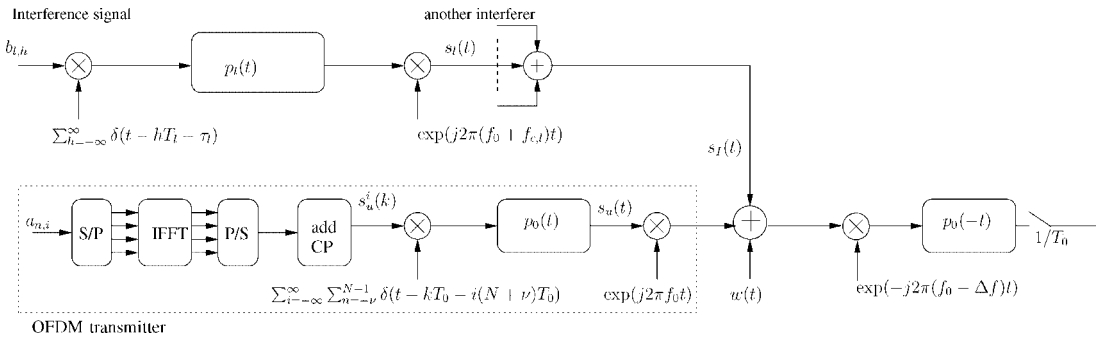

Figure 1. Block diagram of OFDM system including interfering signals.

as interference, and limit the effectiveness of the multi-carrier system. The estimation of the integer part of the CFO may be affected by this NBI. According to our knowledge, no previous research was done to show what is the effect of these NBI signals on the performance of the MC system. This motivates us to study the effect of these NB signals on the different parts of the OFDM receiver. For example, in Reference [11], we have investigated the effect of NBI signals on symbol timing synchronisation for OFDM systems. The result of Reference [11] indicates that the performance of the timing synchroniser is strongly affected by the NBI. It is worth to mention that Caulson investigated the effect of NBI on pilot symbol detection and fractional CFO for OFDM systems in Reference [12]. However, his NBI model was based on an unmodulated complex sinusoid, which is an accurate model for carrier feed-through which arises from I/Q modulators of the transmitter [13]. Although his model describes several sources of NBI, like narrowband FM cordless telephones, baby monitors and garage door openers, it cannot be used for NBI signals with a bandwidth that is larger than a fraction of the MC subcarrier spacing, as e.g. occurs in the B-VHF system [8–10]. Therefore, in this paper, we consider a NBI signal model that is based on a digitally modulated signal and evaluate the effect of these NBI signals on the blind and data aided maximum likelihood (ML) frequency ambiguity estimators in an analytical way. We assume that the fractional part of the CFO can be correctly estimated with another algorithm, and is corrected before the estimation of the integer CFO.

The paper is organised as follows. The system model is addressed in Section 2. In Section 3, we describe the blind and data aided ML integer CFO estimators for OFDM systems. Also, an upper bound on the performance of the estimators is derived in the presence of NBI signals. The simulation and upper bound results are discussed in Section 4. Finally, conclusions are given in Section 5.

2. SYSTEM DESCRIPTION

The basic block diagram of the OFDM system and NBI signal is shown in Figure 1. In the OFDM transmitter, the data stream is grouped in blocks of $2N_u$ data symbols. Next, an N- point inverse fast Fourier transform (IFFT) is performed on each data block, where $N \geqslant 2N_u$[‡], and a cyclic prefix (CP) of length ν is inserted. The kth time domain sample of the ith OFDM block can be written as

$$s_u^i(k) = \sqrt{\frac{1}{N+\nu}} \sum_{n\in I_u} a_{n,i}\, e^{\frac{j2\pi kn}{N}} \qquad -\nu \leqslant k \leqslant N-1 \quad (1)$$

where I_u is a set of $2N_u$ carrier indices and $a_{n,i}$ is the nth data symbol of the ith OFDM block; the data symbols are i.i.d.[§] random values with zero mean and variance $E[|a_{n,i}|^2] = E_s$. The time domain signal of the baseband OFDM signal $s_u(t)$ consists of the concatenation of all time domain blocks $s_u^i(k)$:

$$s_u(t) = \sum_{i=-\infty}^{\infty} \sum_{k=-\nu}^{N-1} s_u^i(k) p_0(t - kT_0 - i(N+\nu)T_0) \quad (2)$$

where $p_0(t)$ is the unit-energy transmit pulse of the OFDM system and $1/T_0$ is the sample rate. The baseband signal (2) is up-converted to the radio frequency f_0. At the receiver, the signal is first down-converted to $-(f_0 - \Delta f)$, where Δf represents the frequency difference between transmitter and receiver oscillator, then fed to the matched filter and finally sampled at rate $1/T_0$. Note that, when the number $2N_u$ of modulated carriers is large, the sample $s_u^i(k)$ consists of a

[‡] As the carriers at the edge of the MC spectrum are more susceptible to disturbances, these carriers are typically not demodulated. These virtual carriers can therefore also serve as a guard band. Hence the number $2N_u$ of used carriers is typically smaller than the FFT size N.

[§] i.i.d. = independently and identically distributed.

DOI: 10.1002/ett

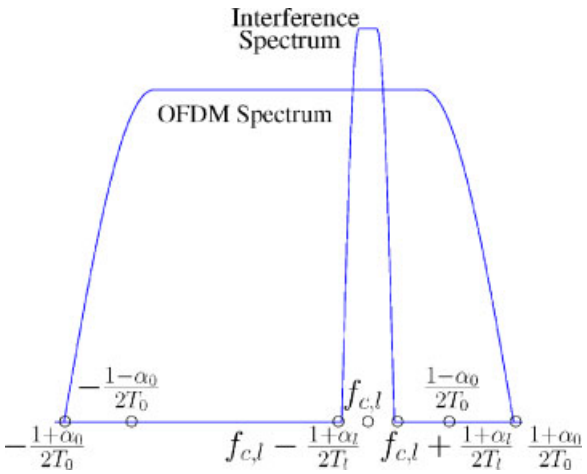

Figure 2. Baseband OFDM and one interfering signal spectrum.

large number of contributions. Hence, taking into account the central limit theorem, the real and imaginary parts of $s_u^i(k)$ can be modelled as Gaussian random variables with zero mean and variance $\sigma_s^2 = (E_s \cdot N_u)/(N+\nu)$. The OFDM signal is disturbed by additive white Gaussian noise with uncorrelated real and imaginary parts, each having variance σ_n^2. The signal to noise ratio (SNR) at the output of the matched filter is defined as σ_s^2/σ_n^2.

Further, the signal is disturbed by narrowband interference residing within the same frequency band as the wideband OFDM signal as shown in Figure 2. To model the interference signal, we follow [11, 14]. The interfering signal $s_I(t)$ is the sum of N_I narrowband interfering signals

$$s_I(t) = \sum_{l=1}^{N_I} s_l(t) \cdot e^{j2\pi(f_0+f_{c,l})t} \tag{3}$$

where $f_{c,l}$ is the carrier frequency deviation from f_0 for the lth interferer and $s_l(t)$ is the lth baseband NBI component that consists of the convolution of a discrete sequence $b_{l,h}$ with the time-domain representation of a transmit pulse $p_l(t)$ as

$$s_l(t) = \sum_{h=-\infty}^{\infty} b_{l,h}\, p_l(t - hT_l - \tau_l) \tag{4}$$

where $b_{l,h}$ is the hth interfering data symbol of the lth interferer, $p_l(t)$ is the unit-energy transmit pulse of the lth interferer, τ_l is its delay, and $1/T_l$ its sample rate. The total NBI signal may be seen at the output of the matched filter of the OFDM receiver as

$$r_I(t) = \sum_{l=1}^{N_I} \sum_{h=-\infty}^{\infty} b_{l,h}\, e^{j2\pi f_{c,l} hT_l}\, g_l(t - hT_l) \tag{5}$$

where $g_l(t)$ is the convolution of $p_0(-t)$ and $p_l(t-\tau_l)\exp(j2\pi(f_{c,l}+\Delta f)t)$. The normalised location of the interferer within the OFDM spectrum may be defined as $f'_{c,l} = ((f_{c,l}+\Delta f)/(B_0))$ where $B_0 = 1/T_0$ is the bandwidth of the OFDM system. It is assumed that the interfering symbols are uncorrelated with each other, i.e. $E[b_{l,h}b^*_{l',h'}] = E'_l\delta_{ll'}\delta_{hh'}$, where E'_l is the energy per symbol of the lth interferer. Further, the interfering data symbols $b_{l,h}$ are statistically independent of the OFDM data symbols $a_{n,i}$. The signal to interference ratio (SIR) at the input of the receiver is defined as [15]

$$\text{SIR} = \frac{2\sigma_s^2/T_0}{\sum_{l=1}^{N_I} \frac{E'_l}{T_l}} \tag{6}$$

3. ML INTEGER CFO ESTIMATOR

As the frequency offset Δf is generally larger than the subcarrier spacing, it is useful to split it into an integer part m and fractional part ϵ, where $\epsilon \in [-0.5, 0.5[$, with respect to the carrier spacing $\delta f = 1/NT_0$, i.e. $\Delta f = m/NT_0 + \epsilon/NT_o$. As in Reference [16], we make the following assumptions:

(1) The parameter ϵ has already been estimated and is perfectly corrected.
(2) A total of N_p pilot symbols are inserted at known locations in each OFDM block. They satisfy the relation $a_{n,0}a^*_{n,1} = d_n\ \forall n \in P$, where d_n is a pseudonoise sequence known at the receiver and P is the set of the pilot-symbol locations (P is empty when $N_p = 0$).
(3) All symbols (known and unknown) belong to a PSK constellation have zero mean and the following second order statistics:

$$E\left[a_{n1,j}a_{n2,f}\right] = 0 \quad -N_u \leqslant n1, n2 < N_u \quad j, f \in \{0,1\} \tag{7}$$

$$E\left[a_{n1,j}a^*_{n2,f}\right] = \begin{cases} 1 & n1 = n2 \quad j = f \in \{0,1\} \\ d_{n1} & n1 = n2 \in P \quad j = 0, f = 1 \\ d^*_{n1} & n1 = n2 \in P \quad j = 1, f = 0 \\ 0 & \text{elsewhere} \end{cases} \tag{8}$$

DOI: 10.1002/ett

We assume that two consecutive OFDM blocks (with indices $i = 0$ and $i = 1$) are observed. The time domain samples outside the CP are given by

$$x_i(k) = e^{j[2\pi(m+\epsilon)(k+i(N+\nu))/N]} s_u^i(k) + w^i(k) + r_I^i(k) \quad (9)$$

where $0 \leqslant k \leqslant N-1$, $i = 0, 1$, $s_u^i(k)$ is given in Equation (1), $w^i(k)$ is the AWGN component and $r_I^i(k)$ is the kth interference sample in the ith block (5).

In this paper, it is assumed that the effect of the fractional frequency offset ϵ/NT_0 is compensated. This is done by rotating the samples $x_i(k)$ in Equation (9) at the angular speed $-2\pi\epsilon/N$ per sample, resulting in samples $z_i(k) = x_i(k)\, e^{-j2\pi\epsilon(k+i(N+\nu))/N}\ \forall\, i = 0, 1$. The rotated samples $z_i(k)$ are fed to an N-point FFT. The nth FFT output of the ith received OFDM block is given by $Z_i(n)$. To estimate m, we use the ML estimator from [16]

$$\hat{m} = \arg \max_{|\tilde{m}| \leqslant M} \{\Lambda(\tilde{m})\} \quad (10)$$

where $\hat{m}$ is the estimated value of m, $\tilde{m}$ is the trial value of m, M represents the largest expected value of $|m|$ and $\Lambda(\tilde{m})$ is given as

$$\Lambda(\tilde{m}) = \sum_{n=-N_u}^{N_u-1} \left[|Z_0(n+\tilde{m})|^2 + |Z_1(n+\tilde{m})|^2 \right] + 2Re \left\{ \sum_{n \in P} d_n Z_0^*(n+\tilde{m}) Z_1(n+\tilde{m}) e^{-j\vartheta(\tilde{m})} \right\} \quad (11)$$

where $\vartheta(\tilde{m}) = 2\pi\tilde{m}(N+\nu)/N$. In the absence of pilot symbols, P is empty and Equation (11) reduces to

$$\Lambda(\tilde{m}) = \sum_{n=-N_u}^{N_u-1} \left[|Z_0(n+\tilde{m})|^2 + |Z_1(n+\tilde{m})|^2 \right] \quad (12)$$

In the following, the estimator corresponding to Equation (12) is referred to as the blind estimator (BE), whereas the estimator corresponding to Equation (11) is called the pilot estimator (PE).

To evaluate the effect of NBI on these estimators, we derive the upper bound on the probability of failure $P_f = Pr\{\hat{m} \neq m\}$ of the estimators. Let $A(\tilde{m}, m)$ be the event that $\Lambda(\tilde{m}) > \Lambda(m)$ where $\tilde{m} \neq m$. Then P_f can be expressed as

$$P_f = Pr \left\{ \bigcup_{\tilde{m}=-M,\, \tilde{m} \neq m}^{M} A(\tilde{m}, m) \right\} \quad (13)$$

This can be upper bounded using the union bound approximation [17],

$$P_f \leqslant \sum_{\tilde{m}=-M,\, \tilde{m} \neq m}^{M} Pr\{\Lambda(\tilde{m}) > \Lambda(m)\} \quad (14)$$

Note that when the number of modulated subcarriers $2N_u$ is large, $\Lambda(\tilde{m})$ consists of a large number of contributions. Hence taking into account the central limit theorem, $\Lambda(\tilde{m})$ can be modelled as a Gaussian random variable. Let us assume $\Lambda(\tilde{m}) \sim N(\mu_{\tilde{m}}, \sigma_{\tilde{m}}^2)^{\|}$, $|\tilde{m}| \leqslant M$ and the covariance between $\Lambda(\tilde{m})$ and $\Lambda(m)$, $\tilde{m} \neq m$ is given by $\sigma_{\tilde{m}m}^2$. We define $H(\tilde{m}, m) = \Lambda(\tilde{m}) - \Lambda(m)$; $H(\tilde{m}, m)$ is a Gaussian random variable with mean $\mu_H(\tilde{m}, m) = \mu_{\tilde{m}} + \mu_m$ and variance $\sigma_H^2(\tilde{m}, m) = \sigma_{\tilde{m}}^2 + \sigma_m^2 - 2\sigma_{\tilde{m}m}^2$. Hence

$$Pr\{\Lambda(\tilde{m}) > \Lambda(m)\} = Q\left(\frac{-\mu_H(\tilde{m}, m)}{\sigma_H(\tilde{m}, m)} \right) \quad (15)$$

Therefore, the upper bound on the probability of failure is given as

$$P_f \leqslant \sum_{\tilde{m}=-M,\, \tilde{m} \neq m}^{M} Q\left(\frac{-\mu_H(\tilde{m}, m)}{\sigma_H(\tilde{m}, m)} \right) \quad (16)$$

where $\mu_H(\tilde{m}, m)$ and $\sigma_H(\tilde{m}, m)$ are derived in the Appendix. In the next section, we will check the validity of the assumptions leading to Equation (16) by means of simulations.

4. NUMERICAL RESULTS

The numerical results in this paper are obtained with the following OFDM and interference parameters:

- Transmit filters are square-root raised-cosine filters with roll off factors $\alpha_0 = 0.25$ and $\alpha_l = 0.5$ for OFDM and interfering signals, respectively.
- The total number of subcarriers is $N = 1024$.

$^{\|}$ $\Lambda(\tilde{m}) \sim N(\mu_{\tilde{m}}, \sigma_{\tilde{m}}^2)$ means that $\Lambda(\tilde{m})$ is Gaussian distributed with average $\mu_{\tilde{m}}$ and variance $\sigma_{\tilde{m}}^2$.

DOI: 10.1002/ett

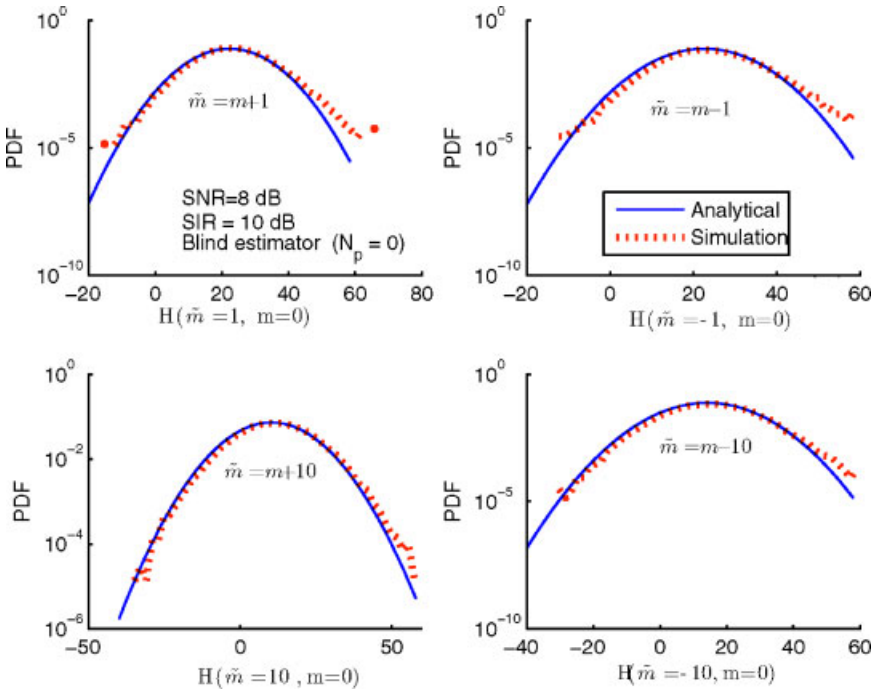

Figure 3. PDF for blind estimator blind ($N_p = 0$) at NBW $= 0.0244$, $f'_{c,1} = 0.5$, and $N_I = 1$.

- The total number of active subcarriers is $2N_u = 1000$. The carriers close to the edge of the OFDM spectrum are not used (virtual carriers).
- The guard interval is set to about 10% of the useful part, $\nu = 102$.
- The bandwidth of the OFDM spectrum, $B_0 = 1/T_0 = 1024$ kHz.
- We use QPSK modulation for the data symbols of the OFDM and the interferer signals.
- The pilot symbols are uniformly distributed over the used carriers.
- The time delay of the interferers $\tau_l = 0$.

Figures 3 and 4 show the simulated PDF and Gaussian approximation of random variable $H(\tilde{m}, m)$ for the blind ($N_p = 0$) and pilot estimators ($N_p \neq 0$), respectively, where we take sample values of $\tilde{m}$ at $\tilde{m} = m \pm 1$ and $\tilde{m} = m \pm 10$. The agreement between the simulated and analytical results assures that $H(\tilde{m}, m)$ can be represented as a Gaussian random variable.

In Figure 5, the probability of failure P_f, based on the obtained upper bound expression (16), is shown as a function of the signal to interference ratio (SIR) for blind ($N_p = 0$) and pilot estimators ($N_p \neq 0$). We have assumed that there is one interference signal ($N_I = 1$) with normalised interference bandwidth, NBW $= B_1/B_0 = 0.0244$ (where $B_1 = 1/T_1$ is the interference bandwidth) and normalised interference frequency $f'_{c,l} = 0.5$. Further, simulation results on the probability of failure are shown. As expected, the pilot estimator ($N_p \neq 0$) outperforms the blind estimator ($N_p = 0$). In the figure, the probability of failure is added for the case where no NBI is present (SIR $= \infty$). At high SIR, the probability of failure clearly converges to the curve corresponding to no NBI; at high SIR, the effect of the NBI diminishes and AWGN dominates. Further, it can clearly be observed that increasing the number of pilot symbols leads to better performance. In our analysis, we have used the union bound approximation to obtain the probability of failure. However, as the metrics $\Lambda(\tilde{m})$ for the true value of $\tilde{m}$ and other values have many common terms, the different hypotheses corresponding to the different values of $\tilde{m}$ are not mutually exclusive. Therefore, the union bound approximation overestimates the true probability of failure, as can be seen in Figure 5, especially for the blind estimation ($N_p = 0$). In the pilot estimator ($N_p \neq 0$), the second term in Equation (11) is dominant, such that the importance of the common terms from the first term in Equation (11) reduces. Therefore, the upper bound for the probability of failure for the pilot estimator is better.

DOI: 10.1002/ett

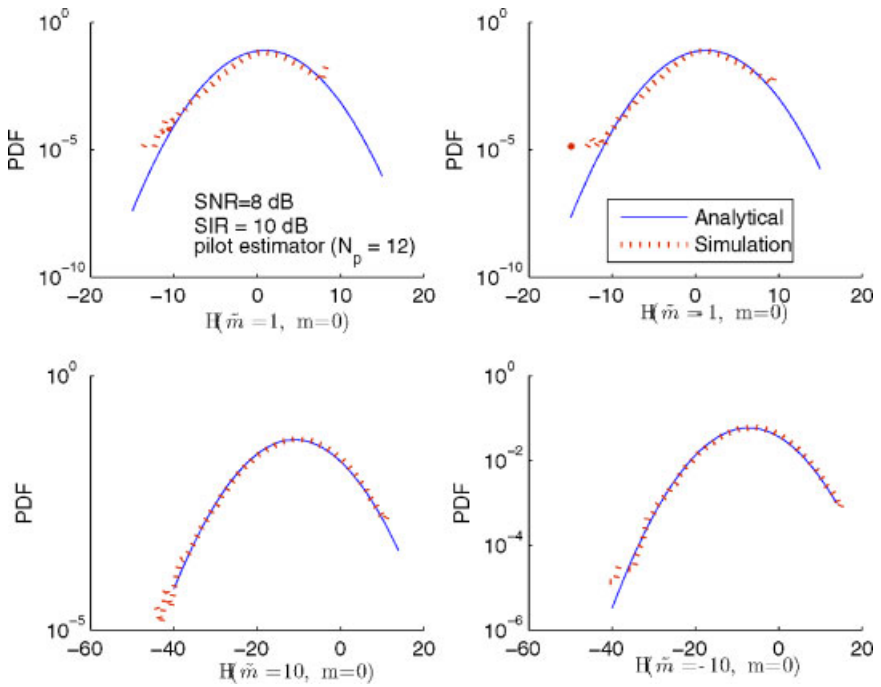

Figure 4. PDF for pilot estimator ($N_p = 12$) at NBW $= 0.0244$, $f'_{c,1} = 0.5$, and $N_I = 1$.

Figure 6 compares the probability of failure P_f obtained with Equation (16) and through simulation, as function of the normalised interference bandwidth (NBW $= B_1/B_0$) for different values of the SIR. We have assumed that SNR $= 8$ dB, $N_I = 1$, $f'_{c,l} = 0.45$. Note that increasing NBW does not have a large influence on P_f, especially at higher values of the SIR. This is explained as, at given SIR, increasing the NBW will cause more carriers to be affected by the NBI, but each carrier will be affected by a smaller amount of interference as the interference power is spread over a larger bandwidth. The net effect is that the performance of the estimator will only slightly depend

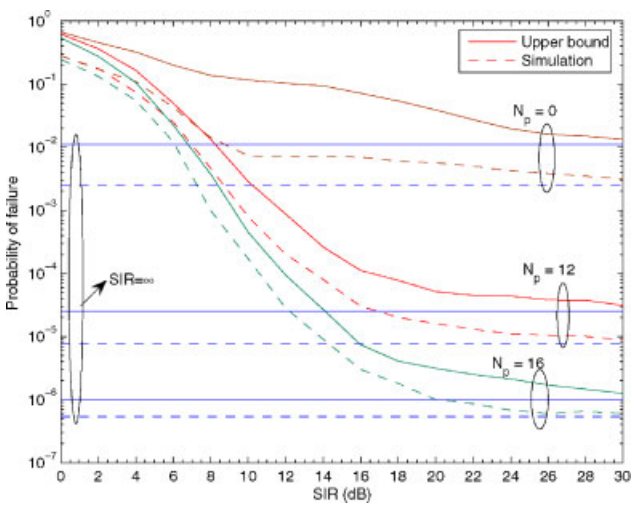

Figure 5. Probability of failure versus signal to interference ratio (SIR) dB, SNR $= 8$ dB, NBW $= 0.0244$, $f'_{c,1} = 0.5$, and $N_I = 1$.

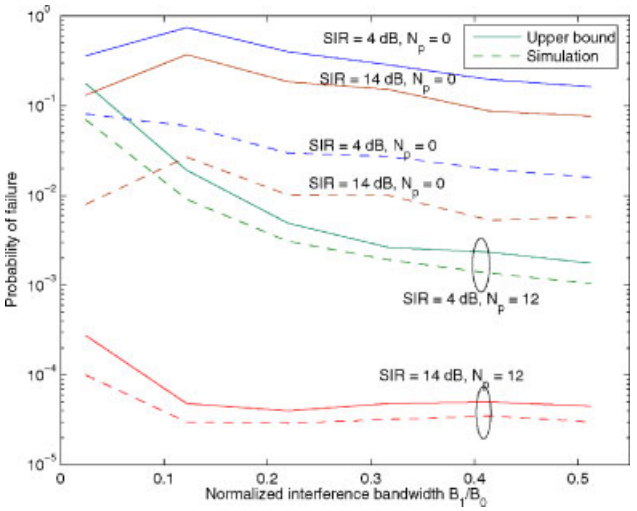

Figure 6. Probability of failure versus normalised interference bandwidth, NBW, $f'_{c,1} = 0.5$ and $N_I = 1$ and SNR $= 8$ dB.

DOI: 10.1002/ett

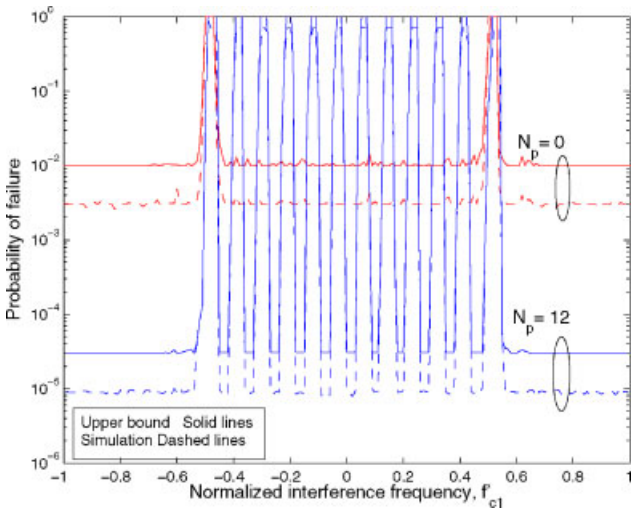

Figure 7. Probability of failure versus normalised interference carrier frequency, $f'_{c,1}$, SIR = 4 dB, SNR = 8 dB, NBW = 0.0244, and $N_I = 1$.

on NBW. Further, at high SIR, the interference signal will diminish and AWGN will dominate. Therefore, it is obvious that at high SIR the performance becomes independent of the NBW.

Figure 7 illustrates the upper bound and simulation results for the probability of failure P_f as function of the normalised interference carrier frequency deviation $f'_{c,1}$ assuming $N_I = 1$ and NBW = .0244. As can be observed, when the NBI signal is located outside the OFDM spectrum, i.e. $|f'_{c,l}| > 0.625$, the position of the interferer has no effect on the estimators. Further, the probability of failure of the blind and the pilot estimator is very sensitive to the location of the interferer within the OFDM spectrum. For the blind estimator, the result indicates that the interference does not have a large effect on P_f as long as the interferer is located within the OFDM spectrum but far away from the region of virtual carriers. This can easily be explained as follows. The blind estimator calculates the sum of the power of the received OFDM subcarriers located in the region $[-N_u, N_u - 1]$ (12) for all $\tilde{m}$, and estimates $\hat{m}$ that maximises $\Lambda(\tilde{m})$ (10). If the interferer is located in the OFDM spectrum but sufficiently far from the virtual carriers, i.e. $|f'_{c,l}| \ll N_u B_0/N$, the interference contribution to $\Lambda(\tilde{m})$ is nearly the same for all values of $\tilde{m}$. Therefore, the NBI will not affect the maximisation of $\Lambda(\tilde{m})$. The worst case scenario occurs when the interferer is located in the virtual carrier region $|f'_{c,l}| \simeq 0.5$. In that case, the optimisation will strongly depend on the position of the interferer as the contribution of the NBI on $\Lambda(\tilde{m})$ will strongly vary as function of $\tilde{m}$. As the probability that an incorrect value of m is selected in the optimisation process is very high in this case, it results in a dramatically increase in P_f. On the other hand, the pilot estimator is very sensitive to the location of NBI within the OFDM spectrum especially at low SIR. This can easily be explained as follows. If the NBI signal is located sufficiently far from the virtual carriers, i.e. $|f'_{c,l}| \ll N_u B_0/N$, the first term in Equation (11) has nearly no effect on the maximisation of $\Lambda(\tilde{m})$ similarly as for the blind estimator. Therefore, the interference contribution to the first term in Equation (11) can be neglected. However, if the interferer is located near a pilot, the interference contribution to the second term in Equation (11) cannot be neglected. As in the simulations we have assumed that the pilots are uniformly distributed over OFDM spectrum, the probability of failure seems a periodic function of the interference frequency. To clearly show the effect of the interferer location within the OFDM spectrum , we enlarge a part of the $f'_{c,l}$ axis as shown in Figure 8. As expected, P_f gets worse when the interferer location approaches the pilot locations. When the SIR increases, it can be seen in Figure 5 that P_f decreases. Hence, for increasing SIR, the value of P_f in Figures 7 and 8 will decrease. For large SIR, the levels will reach a lower limit corresponding to the case of no NBI. Therefore, the difference in the levels, and hence the dependency on the positions of the pilots will decrease when SIR increases, and disappears at high SIR.

Figure 9 shows the upper bound and simulation results for the probability of failure P_f as a function of the number of interfering signals, N_I, in two cases. In case 'A', we

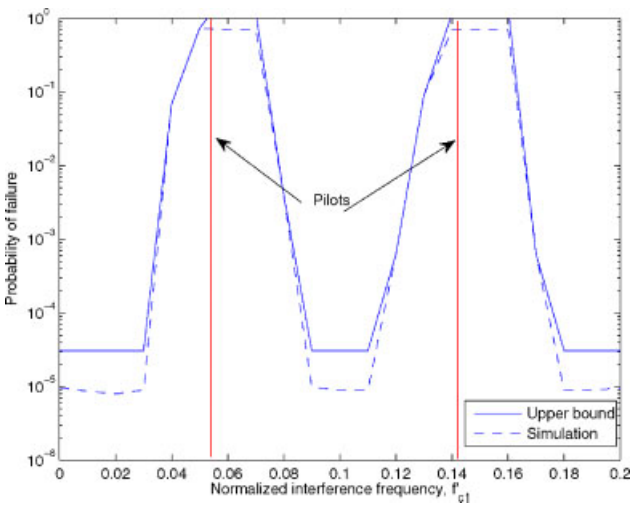

Figure 8. Probability of failure versus normalised interference carrier frequency, $f'_{c,1}$, SIR = 4 dB, SNR = 8 dB, NBW = 0.0244, and $N_I = 1$.

DOI: 10.1002/ett

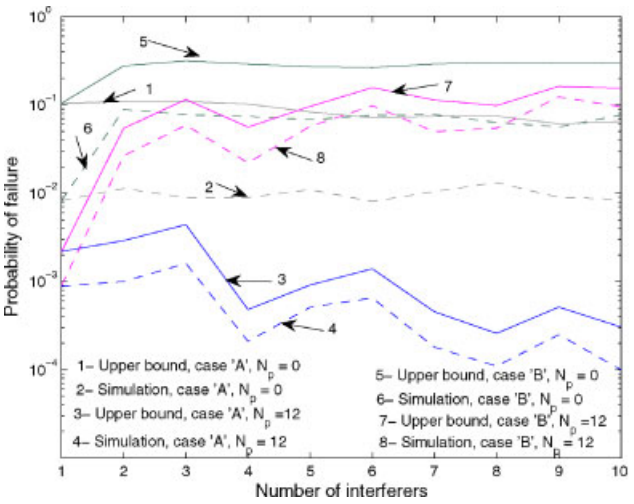

Figure 9. Probability of failure versus number of interference signals, N_I, SIR = 10 dB, NBW = 0.0244 and SNR = 10 dB.

consider a fixed total interference power, hence fixed SIR, i.e. the interference power per interferer decreases linearly as N_I increases. While in case 'B', we consider the case that the interference power, hence SIR, is fixed per interferer, so the total interference power increases proportional to N_I. The location of the interferers is assumed to be uniformly distributed in the region where the OFDM spectrum differs from zero. It is clear that the probability of failure in case 'B' is larger than in case 'A'; the total interference power in the former case is larger than in the latter case. Note that the blind estimator does essentially not depend on the number of interferers for both cases 'A' and 'B'. As the location of the interferer has nearly no effect on the performance of the blind estimator, the number of interferers has nearly no effect on the performance of the blind estimator. For the pilot estimator, the probability of failure only slightly depends on the increasing number of interferers. From Figure 9, we can conclude that the number of interferers has only a small effect on the performance of the estimator.

5. CONCLUSION

This paper evaluates the performance of the blind and pilot maximum likehood frequency ambiguity resolution algorithms in the presence of narrowband interference. An upper bound on the performance of the algorithms is derived, and simulations have been carried out to check the validity of the analytical results. Generally, the bandwidth of the interference and number of interferers do not have a large influence on the performance of the estimators. However, it turns out that the position of the interferers has a large influence of the performance. If the interferer is located in the region of the virtual carriers or, in the case of pilot estimator, close to a pilot symbol, the performance of the estimators is dramatically affected by NBI.

APPENDIX

The nth symbol of the ith received block may be represented as

$$Z_i(n) = Ba_{z,i} + W_i(n) \tag{17}$$

where $B = \sqrt{NE_s/(N+\nu)}$, $z = \text{modulo}(n-m, N)$ and $W_i(n)$ is the total noise resulting from AWGN noise and NBI signals. Using Equations (17) in (11), and after tedious computations, it follows that

$$\mu_{\tilde{m}} = 2B^2 N_p \delta_{\tilde{m}m} + 2B^2 (2N_u + 1 - |m-\tilde{m}|) + \sum_{n=-N_u}^{N_u-1} \chi(n,\tilde{m}) \tag{18}$$

where $\tilde{m} \in [-M, M]$ and $\chi(n,\tilde{m}) = E[|W_0(n+\tilde{m})|^2] + E[|W_1(n+\tilde{m})|^2]$; $E[|W_i(n+\tilde{m})|^2] = 2\sigma_n^2 + \eta_i(n,\tilde{m})$, where $i = 0, 1$, and

$$\eta_i(n,\tilde{m}) = \frac{1}{N} \sum_{k,k'=0}^{N-1} \sum_{l=1}^{N_I} E_l \sum_{h=-\infty}^{\infty} A_l\left(k', h, i\right) A_l^*(k, h, i)\, e^{j2\pi(n+\tilde{m})(k-k')/N} \tag{19}$$

where $A_l(z,h,i) = g_l(zT_0 + i(N+\nu)T_0 - hT_l)$. The variance $\sigma_{\tilde{m}}^2$ is given by

$$\sigma_{\tilde{m}}^2 = (1-\delta_{\tilde{m}m})\,2B^4 N_p + (1+2\delta_{\tilde{m}m})\,2B^2 \sum_{n\in N_P} \chi(n,\tilde{m}) + \sum_{n\in N_P} \psi(n,\tilde{m}) + \sum_{n,n=-N_u}^{N_u-1} \sum_{i=0}^{1} \Phi_i(n,n') + \Omega - \left(\sum_{n=-N_u}^{N_u-1} \chi(n,\tilde{m}) \right)^2 \tag{20}$$

where

$$\Omega = 2B^2 \sum_{n=\max(-N_u,-N_u-m+\tilde{m})}^{\min(N_u-1,N_u-1-m+\tilde{m})} \chi(n,\tilde{m}) \tag{21}$$

DOI: 10.1002/ett

and $\Phi_i(n, n') = E[|W_i(n+\tilde{m})|^2 |W_i(n'+\tilde{m})|^2]$:

$$\begin{aligned}\Phi_i(n, n') = {} & 4\sigma_n^2 \left(\sigma_n^2 + \eta_i(n, \tilde{m})\right) \delta_{nn'} + 4\sigma_n^4 \\ & + 2\sigma_n^2 \left(\eta_i(n, \tilde{m}) + \eta_i(n', \tilde{m})\right) \\ & + 4\sigma_n^2 \eta_i(n, \tilde{m}) \delta_{nn'} + \eta_i(n, \tilde{m}) \eta_i(n', \tilde{m}) \end{aligned} \quad (22)$$

and $\psi(n, \tilde{m}) = E[|W_0(n+\tilde{m})|^2 |W_1(n'+\tilde{m})|^2]$:

$$\begin{aligned}\psi(n, \tilde{m}) = {} & 4\sigma_n^4 + 2\sigma_n^2 \left(\eta_0(n, \tilde{m}) + \eta_1(n, \tilde{m})\right) \\ & + \eta_0(n, \tilde{m}) \cdot \eta_1(n, \tilde{m}) \end{aligned} \quad (23)$$

The covariance $\sigma^2_{\tilde{m}m}$ where $\tilde{m} \neq m$ is given by

$$\begin{aligned}\sigma^2_{\tilde{m}m} = {} & 2B^2 \sum_{n'=-N_u}^{N_u-1} \sum_{n \in P, n=n'+-m+\tilde{m}} \chi(n, \tilde{m}) \\ & + 2B^2 \sum_{n,n'=-N_u, n=n'+m\tilde{-}m}^{N_u-1} \chi(n, \tilde{m}) \\ & + \sum_{n,n'=-N_u}^{N_u-1} \Phi_0(n, n') + \Phi_1(n, n') \\ & - \sum_{n,n'=-N_u}^{N_u-1} \left(2\sigma_n^2 + \eta_0(n, m)\right) \left(2\sigma_n^2 + \eta_0(n', \tilde{m})\right) \\ & - \sum_{n,n'=-N_u}^{N_u-1} \left(2\sigma_n^2 + \eta_1(n, m)\right) \left(2\sigma_n^2 + \eta_1(n', \tilde{m})\right) \end{aligned} \quad (24)$$

ACKNOWLEDGMENT

The first author would like to thank the government of the Arab Republic of Egypt for its funding support.

REFERENCES

1. Bingham JAC. Multicarrier modulation for data transmission: an idea whose time has come. *IEEE Communications Magazine* 1990; **28**(5):5–14.
2. Sari H, Karam G, Jeanclaude I. Transmission techniques for digital terrestial TV broadcasting. *IEEE Communications Magazine* 1995; **33**(2): 100–109.
3. van Nee R, Awater G, Morikura M, Takanashi H, Webster M, Halford KW. New high-rate wireless LAN standards. *IEEE Communications Magazine* 1999; **37**:82–88.
4. Pollet T, Van Bladel M, Moeneclaey M. BER sensitivity of OFDM systems to carrier frequency offset and wiener phase noise. *IEEE Transactions Communications* 1995; **43**(2):191–193.
5. Keller T, Hanzo L. Adaptive multicarrier modulation: a convenient framework for time-frequency processing in wireless communications. *IEEE Proceedings of The IEEE* 2000; **88**:611–640.
6. Zander J. Radio resource management in the future wireless networks: requirements and limitations. *IEEE Communications Magazine* 1997; **35**(8):30–36.
7. Mitola J. Cognitive radio for flexible mobile multimedia communications. In *Proceedings of IEEE International Workshop on Mobile Multimedia Communications*, San Diego, CA, USA, November 1999.
8. Schnell M, Haas E, Sajatovic M, Rihace KC, Haindl B. B-VHF—an overlay system concept for future ATC communications in the VHF band. In *Proceedings of 23-rd DASC*, Salt Lake City, USA, October 2004.
9. Haindl B, Sajatovic M, Rihace KC, Prinz J, Schnell M, Haas F, Cosovic I. B-VHF—a multi-carrier based broadband VHF communications concept for air traffic management. In *Proceedings of IEEE Aerospace Conference*, Big Sky, Montana, USA, March 2005.
10. http://www.b-vhf.org
11. Marey M, Steendam H. Analysis of the narrowband interference effect on OFDM timing synchronization. *IEEE Transactions on Signal Processing* 2007; **55**(9):4558–4566.
12. Coulson AJ. Narrow band interference in pilot symbol assisted OFDM systems. *IEEE Journal on Selected Areas in Communications* 2004; **3**(6):2277–2287.
13. Witrisal K. *OFDM Air-Interface Design for Multimedia Communications*. PhD thesis, Delft Univ. of Technology, 2002.
14. Zhang D, Fan P, Cao Z. Interference cancellation for OFDM systems in presence of overlapped narrow band transmission system. *IEEE Transactions on Consumer Electronics* 2004; **50**(1):108–114.
15. Marey M, Steendam H. The effect of narrowband interference on the timing synchronization for OFDM systems. In *Proceedings of the 12th IEEE Benelux Symposium on Communications and Vehicular Technology*, November 2005.
16. Morelli M, D'Andrea AN, Mengali U. Frequency ambiguity resolution in OFDM systems. *IEEE Communications Letters* 2000; **4**(4):134–136.
17. Proakis JG. *Digital Communications* (3rd edn). McGraw-Hill: New York, USA, 1995.

DOI: 10.1002/ett

AUTHORS' BIOGRAPHIES

Mohamed Marey received the B.Sc. and M.Sc. degrees in Electrical Engineering from Menoufyia University, Menouf, Egypt in 1995 and 1999, respectively. He worked as an Instructor and Assistant Lecturer in the Department of Electronic and Communication Engineering, Menoufyia university in 1996–1999 and 1999–2004, respectively. In 2004, he was granted a fund for scientific research from the government of the Arab Republic of Egypt to prepare Ph.D., towards which he is currently working within the Department of Telecommunications and Information Processing, Ghent University, Belgium. His main research interests include synchronisation, channel estimation, coding and interference cancellation for wireless multi-carrier communication systems. He is the author of several scientific papers in international journals and conference proceedings. He received the young scientist award from International Union of Radio Science (URSI) in 1999.

Heidi Steendam received the M.Sc. degree in Electrical Engineering and the Ph.D. degree in Applied Sciences from Ghent University, Gent, Belgium in 1995 and 2000, respectively. Since September 1995, she has been with the Digital Communications (DIGCOM) Research Group, Department of Telecommunications and Information Processing (TELIN), Faculty of Engineering, Ghent University, Belgium, first in the framework of various research projects, and since October 2002, as a full time Professor in the area of Digital Communications. Her main research interests are in statistical communication theory, carrier and symbol synchronisation, bandwidth-efficient modulation and coding, spread-spectrum (multi-carrier spread-spectrum), satellite and mobile communication. She is the author of more than 80 scientific papers in international journals and conference proceedings. Since 2002, she is an executive Committee Member of the IEEE Communications and Vehicular Technology Society Joint Chapter, Benelux Section. She has been active in various international conferences as Technical Program Committee member and Session chair. In 2004, she was the conference chair of the IEEE Symposium on Communications and Vehicular Technology in the Benelux. She is teaching courses on Data Communications, Information Theory and Advanced Modulation and Coding Techniques.

DOI: 10.1002/ett